Chapter 15

Fabrication of Hydrogenated Diamond Metal–Insulator–Semiconductor Field-Effect Transistors

Jiangwei Liu and Yasuo Koide

Abstract

Diamond is regarded as a promising material for fabrication of high-power and high-frequency electronic devices due to its remarkable intrinsic properties, such as wide band gap energy, high carrier mobility, and high breakdown field. Meanwhile, since diamond has good biocompatibility, long-term durability, good chemical inertness, and a large electron-chemical potential window, it is a suitable candidate for the fabrication of biosensors. Here, we demonstrate the fabrication of hydrogenated diamond (H-diamond) based metal–insulator–semiconductor field-effect transistors (MISFETs). The fabrication is based on the combination of laser lithography, dry-etching, atomic layer deposition (ALD), sputtering deposition (SD), electrode evaporation, and lift-off techniques. The gate insulator is high-k HfO_2 with a SD/ALD bilayer structure. The thin ALD-HfO_2 film (4.0 nm) acts as a buffer layer to prevent the hydrogen surface of the H-diamond from plasma discharge damage during the SD-HfO_2 deposition. The growth of H-diamond epitaxial layer, fabrication of H-diamond MISFETs, and electrical property measurements for the MISFETs is demonstrated. This chapter explains the fabrication of H-diamond FET based biosensors.

Key words H-diamond, MISFET, high-k, SGFET, Biosensor

1 Introduction

Semiconductor ion-sensitive field-effect transistor (ISFET) and dielectric-modulated metal–insulator–semiconductor FET (DM-MISFET) based biosensors have received much attention due to their high sensitivity, label-free detection, and high scalability [1, 2]. Figure 1 schematically illustrates the (a) ISFET and (b) DM-MISFET. The device structure of ISFET is similar to that of the MISFET. The difference between them is that the gate metal for the MISFET is replaced by an electrolyte for the ISFET. Since it is difficult to detect neutral biomolecules and there is a lack of compatibility with standard complementary metal–oxide–semiconductor (CMOS) technology for the ISFET biosensors, the DM-MISFET biosensors have been developed. The DM-MISFET has nano-gaps between the insulator and gate metal, which is

Ben Prickril and Avraham Rasooly (eds.), *Biosensors and Biodetection: Methods and Protocols, Volume 2: Electrochemical, Bioelectronic, Piezoelectric, Cellular and Molecular Biosensors*, Methods in Molecular Biology, vol. 1572,
DOI 10.1007/978-1-4939-6911-1_15,

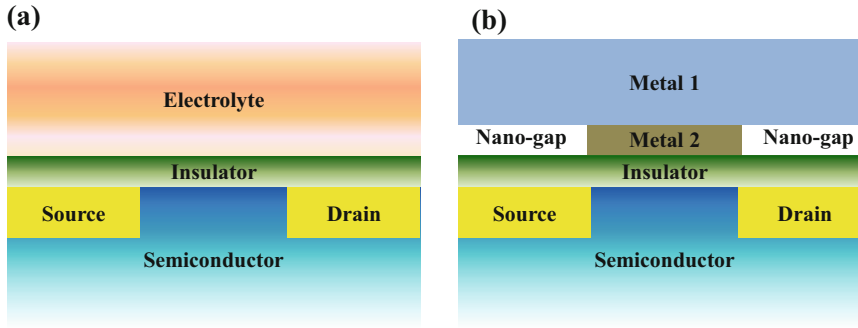

Fig. 1 Schematic diagrams of the (**a**) ISFET and (**b**) DM-MISFET

formed by an etching process. It has good compatibility with the CMOS process and provides a useful approach to neutral biomolecular detection.

Diamond has a wide band gap of 5.47 eV, large thermal conductivity, high breakdown field, large saturation velocity, and high carrier mobility. It is considered a suitable semiconductor for fabrication of high-power, high-frequency, and high-temperature electronic devices. Since diamond has good biocompatibility, long-term durability, good chemical inertness, and a large electron-chemical potential window, it is a suitable candidate for the fabrication of biosensors. Because activation energies of diamond-dopants (370 and 570 meV for boron and phosphorus doped diamond, respectively) are much higher than room temperature thermal energy (26 meV), an available diamond channel layer is necessary for the fabrication of diamond-based electronic and bioelectronics devices. Hydrogenated diamond (H-diamond) can accumulate holes on the surface with sheet hole density and mobility of ~10^{12} to 10^{13} cm^{-2} and ~100 $cm^2 \cdot V^{-1} \cdot s^{-1}$, respectively. After exposing H-diamond to ambient NO_2, the hole density of the H-diamond channel layer may increase to as high as ~10^{14} cm^{-2} ([3]). Therefore H-diamond is considered to be a good channel layer for fabricating high-performance diamond-based electronic and bioelectronics devices. H-diamond solution-gate FET (SGFET) biosensors have recently been reported [4, 5]. Since H-diamond it does not require a passivation layer, H-diamond SGFET biosensors are more sensitive than Si-based ISFET biosensors. Although the DM-MISFET biosensors are believed to be capable of detecting neutral biomolecules, there are few reports of fabrication of H-diamond-based DM-MISFET biosensors.

In order to fabricate H-diamond SGFET and DM-MISFET biosensors it is to understand H-diamond FET fabrication. In our previous studies, we focused on the fabrication of high-*k*/H-diamond MISFETs [6, 7]. The high-*k* insulators can respond to the high hole density (~10^{14} cm^{-2}) of the NO_2-treated H-diamond channel layer at a low gate electrical field. They are deposited by

atomic layer deposition (ALD) and sputtering deposition (SD) techniques with a SD/ALD bilayer structure. The thin ALD-insulator impacts as a buffer layer to prevent the hydrogen surface of the H-diamond from plasma discharge damage during the SD-insulator deposition. Here, we will demonstrate the growth of H-diamond epitaxial layer, fabrication details of the SD-HfO_2/ALD-HfO_2/H-diamond MISFETs, and electrical property measurement for the MISFETs.

2 Materials

2.1 H-Diamond Epitaxial Layer Growth

1. Diamond substrate (Ib-type single crystalline diamond (001), dimension: 2.5 × 2.5 × 0.5 mm; Sumitomo Electric Industries, Ltd., Osaka, Japan).
2. Sulfuric acid (Concentration: 98%; Kishida Chemical Corp., Ltd., Osaka, Japan).
3. Nitric acid (Concentration: 69%; Kishida Chemical Corp., Ltd., Osaka, Japan).
4. Hotplate (Model No.: C-MAG HP 10-S27, heat output: 1050 W, heat temperature range: 50–500 °C, heat rate: 5 K/min, dimension: 300×105×415 mm, voltage: 100 V, frequency: 50/60 Hz; IKA Japan, Osaka, Japan).
5. Methanol (Concentration: >99.8%; Kishida Chemical Corp., Ltd., Osaka, Japan).
6. Acetone (Concentration: >99.5%; Kishida Chemical Corp., Ltd., Osaka, Japan).
7. Microwave plasma-enhanced chemical vapor deposition system (MPCVD, Model No.: AX5200S; Seki Technotron Corp., Tokyo, Japan).
8. MPCVD microwave plasma generator (Model No.:AX3120, power: 1500 W; ASTex Applied Science and Technology, Inc., Wilmington, MA, U. S. A.).
9. Hydrogen diffusion purifier (Model No.:LS-2, rate of flow: 300 L./h, pressure:0.98 MPa; Japan Pionics Co., Ltd., Tokyo, Japan).
10. Methane gas (Purity: >99.999%; Japan Fine Products, Kanagawa, Japan).
11. Hydrogen gas (Purity: >99.999%; Air Water Hydrogen Corp., Tokyo, Japan).
12. Pocket digital multimeter (Yokogawa Meters & Instruments Corp., Tokyo, Japan).

2.2 MISFET Fabrication

1. Photoresist: LOR 5A (Nippon Kayaku Corp. Ltd., Tokyo, Japan).
2. Photoresist: AZ5214E (AZ Electronic Materials USA Corp., U. S. A.).
3. Photoresist developing solution: Tetramethylammonium hydroxide (TMAH, concentration: 2.38%; AZ Electronic Materials USA Corp., U. S. A.).
4. Spin-coater (Model No.: Opticoat MS-A150; Mikasa Corp., Ltd., Tokyo, Japan).
5. Photoresist baking hotplate (Model No.: Digital hotplate NINOS ND-1; AS ONE Corp., Osaka, Japan).
6. AR_CAD software (System House Fukuchiyama Corp., Ltd., Kyodo, Japan).
7. Layout Editor software (Build: 20,080,205, Author: Jürgen Thies; hompage: http://layout.sourceforge. net).
8. Laser lithography system (Light source: semiconductor laser with wavelength of 405 nm, light intensity of 300 mW/cm^2; Nanosystem Solutions, Inc., Okinawa, Japan).
9. Microscope (Model No.: BX51M; Olympus Corp., Tokyo, Japan).
10. Mount adaptor (Model No.: U-TV0.5XC-3; Olympus Corp., Tokyo, Japan).
11. Capacitive coupled plasma (CCP) dry-etching system (SAMCO International Inc., Kyoto, Japan).
12. Electron-gun (E-gun) evaporation system (Model No.: RDEB-1206 K; R-DEC Corp., Ltd., Ibaraki, Japan).
13. E-gun evaporation targets: Gold/titanium/palladium (Au/Ti/Pd, Kojundo Chemical Lab. Corp., Ltd., Saitama, Japan).
14. Atomic layer deposition system (Model No.: SUNALE R-100B, Picosun Altech Corp., Ltd., Tokyo, Japan).
15. $Hf[N(C_2H_5)CH_3]_4$ precursor (Tri Chemical Laboratories Inc.,Yamanashi, Japan).
16. Water vapor precursor (Tri Chemical Laboratories Inc., Yamanashi, Japan).
17. ALD carrier gas: N_2 (Japan Fine Products, Kanagawa, Japan).
18. Radio-frequency (RF) sputtering deposition (SD) system (Handmade).
19. HfO_2 target for RF-SD system (Purity: >99%, Furuuchi Chemical Corp., Tokyo, Japan).
20. RF generator (Model No.:T847 M, Biemtron Co., Ltd., Tsukuba, Japan).
21. Argon gas (Japan Fine Products, Kanagawa, Japan).

22. Ellipsometer (Model No.: Mary-102, 5Lab Corp., Ltd., Saitama, Japan).
23. N-methyl-2-pyrrolidone solution (NMP; Wako Pure chemical Industries, Ltd., Osaka, Japan).
24. Ethanol (Wako Pure chemical Industries, Ltd., Osaka, Japan).
25. Acetone (Wako Pure chemical Industries, Ltd., Osaka, Japan).
26. Manual probe system (Prober model MX-200/B; Vector Semiconductor Corp., Ltd., Tokyo, Japan).
27. Analyzer of manual probe system (Model No.: B1500A; Agilent Technologies Inc., Tokyo, Japan).

3 Methods

3.1 H-diamond Epitaxial Layer Growth

3.1.1 Diamond Substrate Surface Treatment

Before the H-diamond growth, the Ib-type single crystalline diamond (001) substrate is boiled using a hotplate in a mixture H_2SO_4 and HNO_3 solutions at 300 °C for 3 hours. The volume ratio between H_2SO_4 and HNO_3 is 1:1. Figure 2 shows the images of (a) digital hotplate and (b) diamond substrate treatment using hotplate at 300 °C.

(a) The hotplate power is turned on and the temperature is adjusted to 300 °C (*see* **Note 1**).

(b) The diamond substrate is put in the bottom of a beaker. The HNO_3 and H_2SO_4 solutions are poured into the beaker sequentially with the volume ratio of 1:1 (*see* **Note 2**).

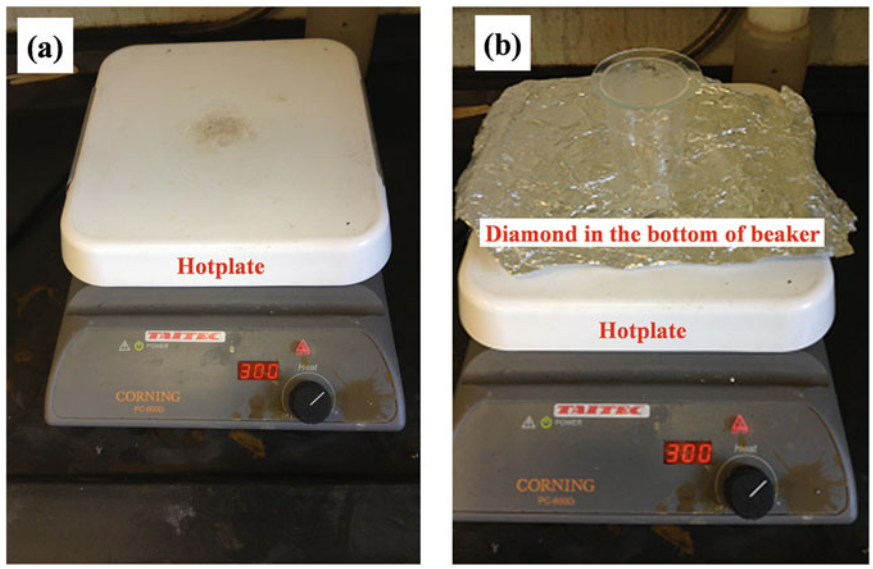

Fig. 2 Images of (**a**) digital hotplate and (**b**) diamond substrate treatment using hotplate at 300 °C. The diamond substrate is located at the bottom of the beaker

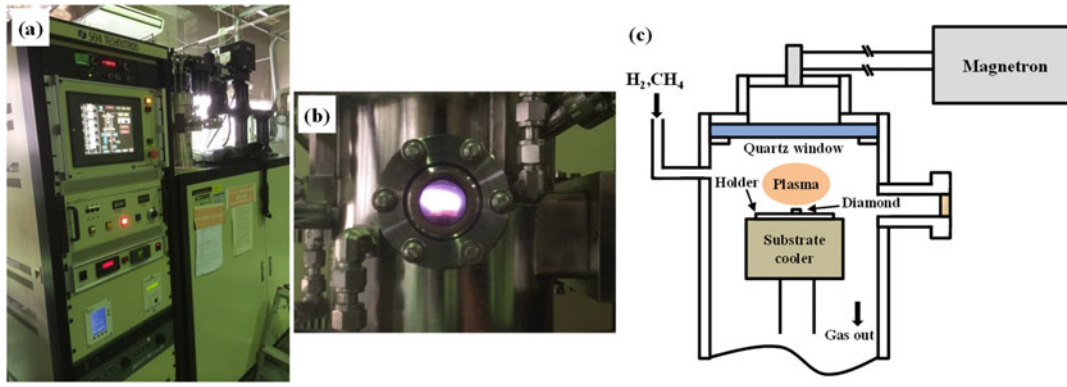

Fig. 3 Images of (**a**) MPCVD and (**b**) H-diamond growth using the MPCVD, and (**c**) schematic diagram of the H-diamond growth using the MPCVD

(c) After waiting the hotplate temperature up to 300 °C, the beaker is moved onto the hotplate (*see* **Note 3**).

(d) After boiling for 3 h, the diamond is cleaned ultrasonically using deionized water, acetone, methanol, and deionized water sequentially. The cleaning time of diamond substrate in each solution is 5 min.

(e) The diamond substrate is blow-dried by argon gas finally.

3.1.2 H-diamond Epitaxial Layer Growth

The H-diamond epitaxial layer is grown on the Ib-type single crystalline diamond (001) substrate by the MPCVD system. Figure 3 shows the images of (a) MPCVD and (b) H-diamond growth using the MPCVD, and (c) schematic diagram of the H-diamond growth using the MPCVD. There is a quartz window on the top of the chamber. The diamond substrate is set on the holder. The height of the holder can be adjusted by a driving motor.

(a) The cooling water, H_2 gas, and CH_4 gas are opened.

(b) The diamond substrate is led into the MPCVD chamber.

(c) The mechanical and turbo molecular pumps are turned on sequentially. It is necessary to wait about 1 h for the chamber vacuum lower than 5×10^{-7} Torr.

(d) The holder height is adjusted to 28.0 mm.

(e) The H_2 gas is purified by the hydrogen diffusion purifier.

(f) After waiting the chamber vacuum lower than 5×10^{-7} Torr, the turbo molecular and mechanical pumps are turned off sequentially.

(g) The purity hydrogen gas is led into the MPCVD chamber with the flow rate of around 30 sccm.

(h) The microwave power is turned on and is adjusted to around 100~200 W. The hydrogen plasma is built up.

(i) The microwave power is increased to around 1100~1200 W. Meanwhile, the flow rate of H_2 gas is adjusted to 500 sccm.

(j) The chamber pressure is fixed at 80 Torr. The reflected power is adjusted to be lower than 3 W. The diamond surface temperature is around 1000 °C.

(k) The H-diamond surface is cleaned for 20 min at high temperature of around 1000 °C.

(l) The microwave power is decreased to be around 900~960 W. The surface temperature of the diamond substrate is in the range of 900~940 °C (*see* **Notes 4** and **5**).

(m) The CH_4 gas is led into the MPCVD chamber with the flow rate of 0.5 sccm (*see* **Note 6**).

(n) The H-diamond epitaxial layer growth is begun. The deposition time and thickness of the H-diamond epitaxial layer are around 1.5~2 h and 150~200 nm, respectively (*see* **Notes** 7 and **8**).

(o) After finishing the H-diamond growth, the microwave power is turned off, and the CH_4 gas is stopped.

(p) It is necessary to wait around 1 h to decrease the holder temperature to room temperature.

(q) The H_2 gas is stopped.

(r) The sample is taken out from the chamber.

(s) The H_2 gas, CH_4 gas, and cooling water are closed.

(t) It is important to confirm whether there is surface channel layer for the H-diamond epitaxial layer. The resistance of the H-diamond is measured by a pocket digital multimeter. The resistance should be in the range of 10 kΩ~500 kΩ (*see* **Notes 9** and **10**).

3.2 Fabrication and Characterization of SD-HfO_2/ALD-HfO_2/H-Diamond MISFETs

The fabrication of SD-HfO_2/ALD-HfO_2/H-diamond MISFETs is based on the combinations of laser lithography, dry-etching, ALD, SD, electrode evaporation, and lift-off techniques. The electrical properties of the MISFETs are measured by a manual probe system. Figure 4 shows the fabrication process of the MISFET. There are three major steps: mesa-structure formation [Fig. 4a], gate oxide and contact formation [Fig. 4b], and source/drain ohmic contact formation [Fig. 4c].

3.2.1 Laser Lithography System

(a) The sample is coated using the spin-coater with positive photoresists of LOR5A and AZ5214E sequentially. The rotation rate and time for both photoresists are 7000 rpm and 1 s, respectively. The baking temperature and time for the LOR

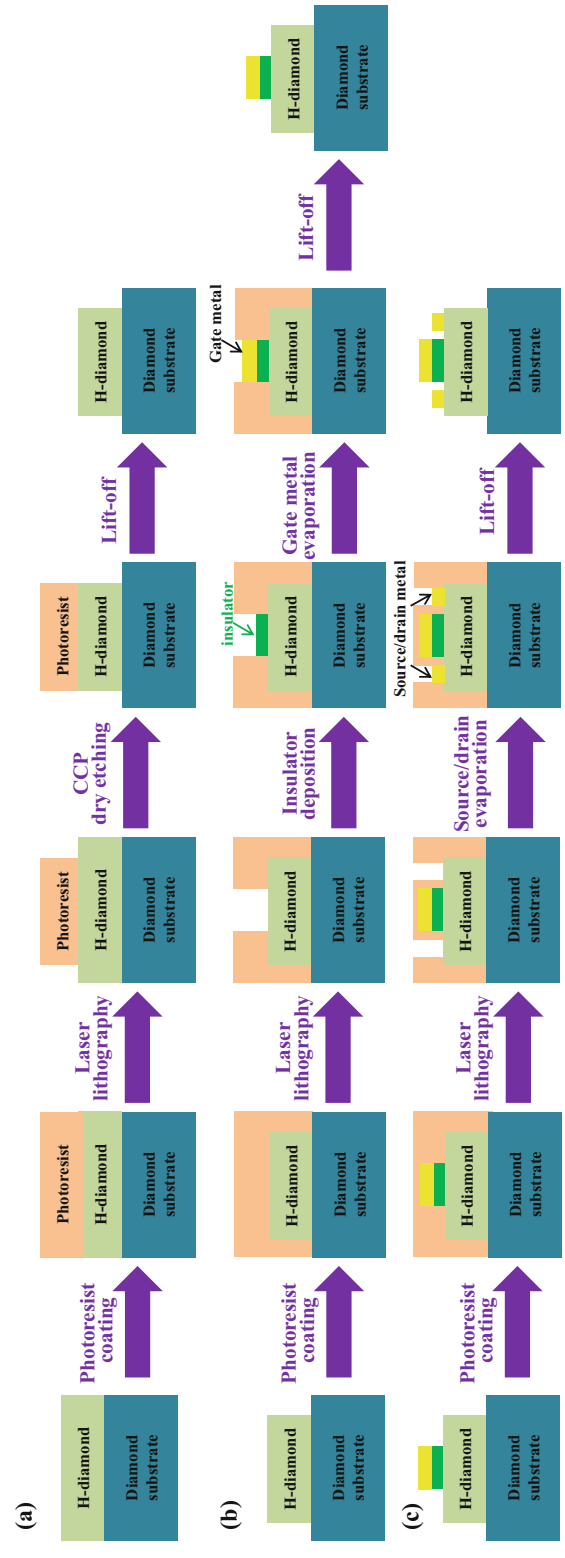

Fig. 4 Outline of the process used to fabricate H-diamond MISFET: (**a**) mesa-structure formation, (**b**) gate insulator and metal contact formation, and (**c**) source/drain ohmic contact formation

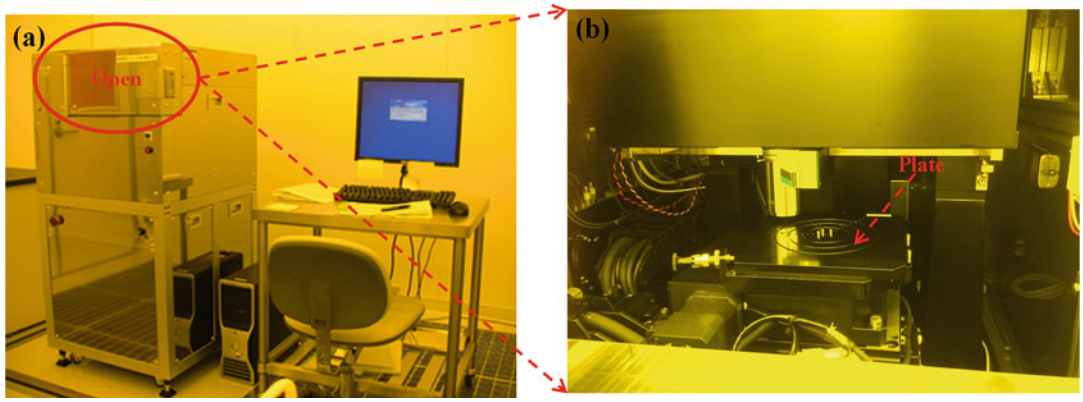

Fig. 5 Images of (**a**) laser lithography system and (**b**) opening state of the laser lithography system

5A are 180 °C and 5 min, respectively. Those for the AZ5214E are 110 °C and 2 min, respectively (*see* **Note 11**).

(b) The patterns of the sample are formed using DL-1000 laser lithography system, which is shown in Fig. 5a. The patterns can be designed using the Layout Editor and AR_CAD software (*see* **Note 12**).

(c) The plate is used to set the sample [Fig. 5b]. The total height of the plate and diamond substrate is around 9.0 mm.

(d) The sample is exposed by the semiconductor laser with wavelength of 405 nm. The expose dose of the laser is around 200~250 mJ/cm^2 with 4 frames per second.

(e) After exposing the photoresists using the laser lithography system, the sample is developed in the TMAH solution for 2.5 min.

(f) The sample is cleaned in the deionized water for 20~30 s.

(g) It is necessary to check whether the exposed photoresists have been removed totally using the microscope (*see* **Note 13**).

3.2.2 CCP Dry-Etching System

The mesa-structure of the sample is formed using CCP dry-etching system.

(a) The O_2 etching gas is opened.

(b) The chamber is cleaned using O_2 for 15 min.

(c) The sample is led into the etching chamber.

(d) The etching conditions are set up. The pressure and etching time are 10 Pa and 90 s, respectively. The O_2 flow rate and plasma power are 100 sccm and 50 W, respectively (*see* **Note 14**).

(e) The etching process can be performed automatically with the setting conditions.

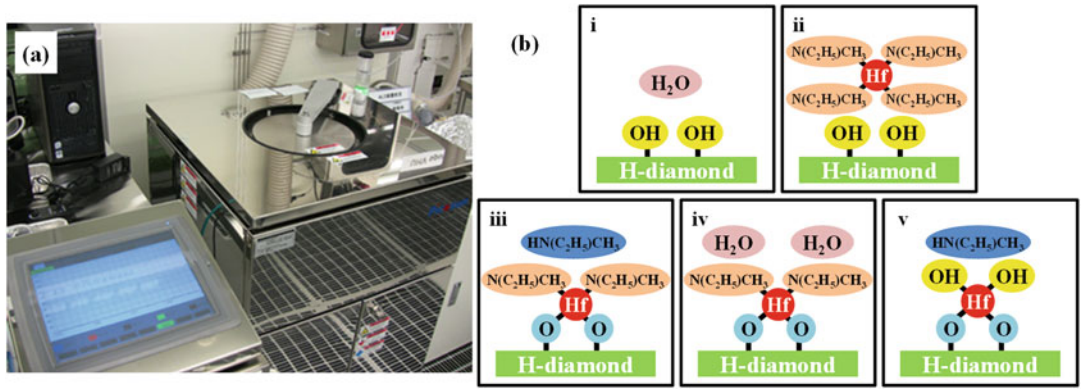

Fig. 6 (**a**) Image of ALD equipment and (**b**) outline of the ALD-HfO_2 formation using $Hf[N(C_2H_5)CH_3]_4$ and water vapor

(f) After finishing the etching process, the sample is taken out from the chamber (*see* **Note 15**).

(g) The O_2 etching gas is closed.

3.2.3 ALD-HfO_2 Deposition

After forming the mesa-structure, it is necessary to form the pattern again using the laser lithography system for the gate oxide insulators and contact formation. The ALD-HfO_2 buffer layer is deposited at 120 °C with precursors of $Hf[N(C_2H_5)CH_3]_4$ and water vapor. The image of the ALD equipment is shown in Fig. 6a. The ALD is a thin film deposition technique. This technique is based on the sequential use of a gas phase chemical process. Figure 6b shows the HfO_2 deposition using the ALD with $Hf[N(C_2H_5)CH_3]_4$ and water vapoer as precursors. At first, the water vapor enters the chamber, and there are -OH bonds formed on the surface of H-diamond [Fig. 6 (b)-i]. Then, $Hf[N(C_2H_5)CH_3]_4$ reacts with surface –OH to form –Hf–O– bonds on the H-diamond [Fig. 6b-ii and iii]. Pulse water vapor into the chamber again to remove the $HN(C_2H_5)CH_3$ groups and to create –Hf–OH bonds [Fig. 6 (b)-iv and v].

(a) The N_2 carrier gas is opened.

(b) The heating temperature for the $Hf[N(C_2H_5)CH_3]_4$ precursor is increased with three steps. The first setting temperature is 100 °C with the heater temperature and waiting time of 115 °C and 1 h, respectively. The second setting temperature is 115 °C with the heater temperature and waiting time of 130 °C and 1 h, respectively. The third setting temperature is 128 °C with the heater temperature and waiting time of 160 °C and 1 h, respectively (*see* **Note 16**).

(c) The sample is led into the ALD chamber.

(d) The deposition receipt is designed. The pulse and purge times for both water vapor and $Hf[N(C_2H_5)CH_3]_4$ precursors are 0.1 and 4.0 s, respectively (*see* **Note 17**).

(e) After opening the water vapor and $Hf[N(C_2H_5)CH_3]_4$ precursors sequentially, the deposition of ALD-HfO_2 starts.

(f) The deposition rate of the ALD-HfO_2 is around 1.25 Å/cycle. The total deposition cycles and the thickness of the ALD-HfO_2 buffer layer are 32 cycles and 4.0 nm, respectively.

(g) After finishing the ALD-HfO_2 deposition, the $Hf[N(C_2H_5)CH_3]_4$ and water vapor precursors are closed sequentially.

(h) The sample is taken out from the chamber (*see* **Note 18**).

(i) The carrier gas of N_2 is closed finally.

3.2.4 SD-HfO_2 Deposition

The SD-HfO_2 layer is deposited in a pure argon ambient at room temperature. The image of our handmade RF-SD equipment and the schematic diagram of it are shown in the Fig. 7.

(a) The cold water and the argon gas are opened.

(b) The sample is set on the holder and is led into the load-lock chamber.

(c) After waiting 15 min, the sample is transferred from load-lock chamber to main chamber.

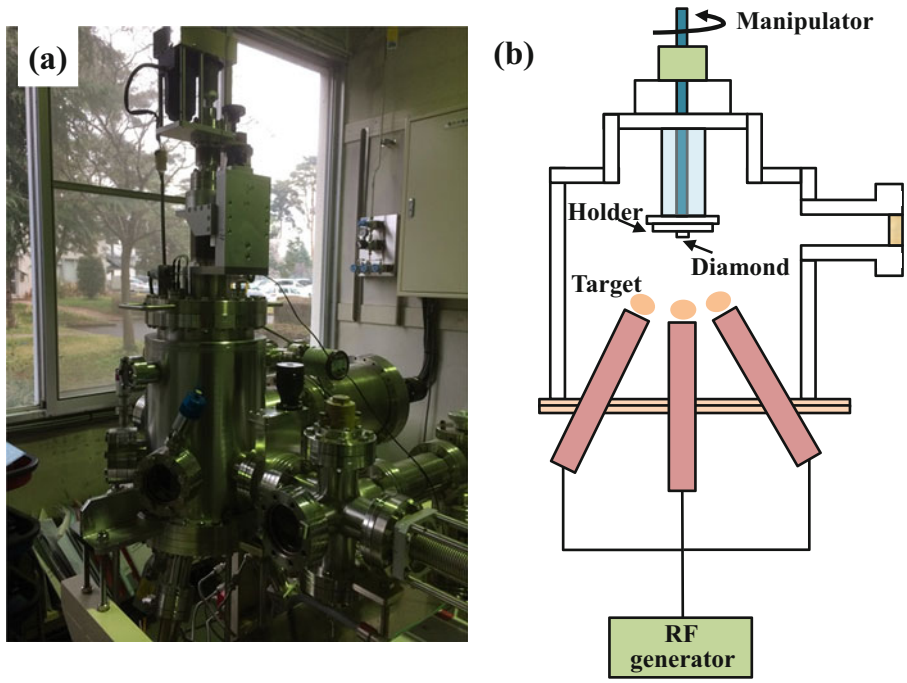

Fig. 7 (**a**) Image of our handmade RF-SD equipment and (**b**) schematic diagram of it

(d) The flow rate of argon gas is adjusted to 10 sccm, and the chamber pressure is around 5 Pa.

(e) The RF generator power is turned on and adjusted to 30 W, and the luminance of SD-HfO_2 target is built up.

(f) The flow rate of argon gas is decreased to 2 sccm. The chamber pressure is kept at 1 Pa.

(g) The deposition of SD-HfO_2 is begun (*see* **Note 19**).

(h) The deposition rate of the SD-HfO_2 is around 1.5 nm/min.

(i) After finishing the deposition of SD-HfO_2, the power is turned off, and the sample is transferred from main chamber to load-lock chamber.

(j) The sample is taken out from the load-lock chamber.

(k) The cold water and the argon gas are closed.

(l) Thickness of the SD-HfO_2 is around 8.6 nm (*see* **Note 20**).

3.2.5 Evaporation System for Electrodes Formation

The gate metal and source/drain ohmic contacts are formed using E-gun evaporation system. The metal components for all the contacts are Au/Ti/Pd (200/20/10 nm), where the slash "/" indicates the stack sequence from the top surface.

(a) The diamond substrate is stuck on the holder and is led into the load-lock chamber of E-gun evaporation system.

(b) After waiting for the load-lock chamber pressure to lower to 7×10^{-3} Pa, the sample is transferred into the main evaporation chamber (*see* **Note 21**).

(c) The power for the evaporation system is turned on. The current is increased gradually to enhance the metal evaporation rate.

(d) The Pd metal is evaporated first. The evaporation rate is 0.5 Å/s (*see* **Note 22**).

(e) The Ti metal is evaporated second. The evaporation rate is 0.5 Å/s (*see* **Note 22**).

(f) The Au metal is evaporated last. The evaporation rate is 2.0 Å/s (*see* **Note 22**).

(g) After finishing the evaporation, the sample is transferred from the main chamber to load-lock chamber.

(h) The sample is taken out from the load-lock chamber.

3.2.6 Photoresist Lift-Off Process

(a) The photoresists are lifted-off by immersing the sample in the NMP solution.

(b) The lift-off temperature is room temperature (*see* **Note 23**).

(c) The lift-off time is 30 min for the mesa-structure formation step [Fig. 4a]. It is 3 h for the gate and source/drain contacts formation steps [Figs. 4b, c].

(d) After 30 min or 3 h lifting-off, the sample is washed using a syringe with the NMP solution (*see* **Note 24**).

(e) The sample is cleaned using acetone and ethanol sequentially (*see* **Note 25**).

(f) The sample is blow-dried using argon gas.

(g) It is necessary to check whether the photoresists have been removed totally using the Microscope.

3.2.7 Electrical Property Measurement for the MISFETs

The schematic interfacial structure of the MISFET is shown in the Fig. 8. The gate width (W_G) is fixed at 150 μm with the gate length (L_G) of 4 μm. The inner distance between the gate electrode edge and the oxide layer is kept at 10 μm. The electrical properties of the SD-HfO_2/ALD-HfO_2/H-diamond MISFETs are measured under a dark condition using high performance MX-200/B prober and B1500A parameter analyzer. The measurement temperature is room temperature.

(a) The sample is fixed on the measurement stage.

(b) The measurement probes contact with gate, source, and drain electrodes.

(c) The source–drain current versus source–drain voltage (I_{DS}-V_{DS}) and source–drain current versus gate voltage (I_{DS}-V_{GS}) have been measured.

(d) For the I_{DS}-V_{DS} measurement, the V_{GS} is varied from −4 to 2 V in steps of +0.5 V, and the V_{DS} is varied from 0 to −5 V in steps of −0.1 V. For the I_{DS}-V_{GS} measurement, the V_{DS} is fixed at −4 V, and the V_{GS} is varied from 0 to −6 V in steps of −0.1 V.

(e) Figure 9a shows the I_{DS}-V_{DS} for the SD-HfO_2/ALD-HfO_2/H-diamond MISFET. The MISFET shows good operation and *p*-type channel characteristic. The maximum I_{DS} value for the MISFET is −15.1 mA/mm

(f) Figure 9b shows transfer characteristic corresponding to the I_{DS}-V_{DS}. The threshold voltage (V_{TH}) is determined to be −0.2 ±0.1 V at the V_{DS} of −4 V. The SD-HfO_2/ALD-HfO_2/H-diamond MISFET shows enhancement-mode

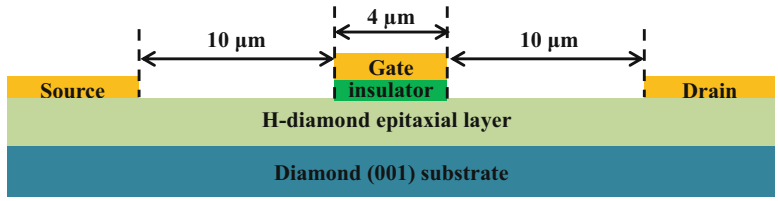

Fig. 8 Schematic interfacial structure of the SD-HfO_2/ALD-HfO_2/H-diamond MISFET

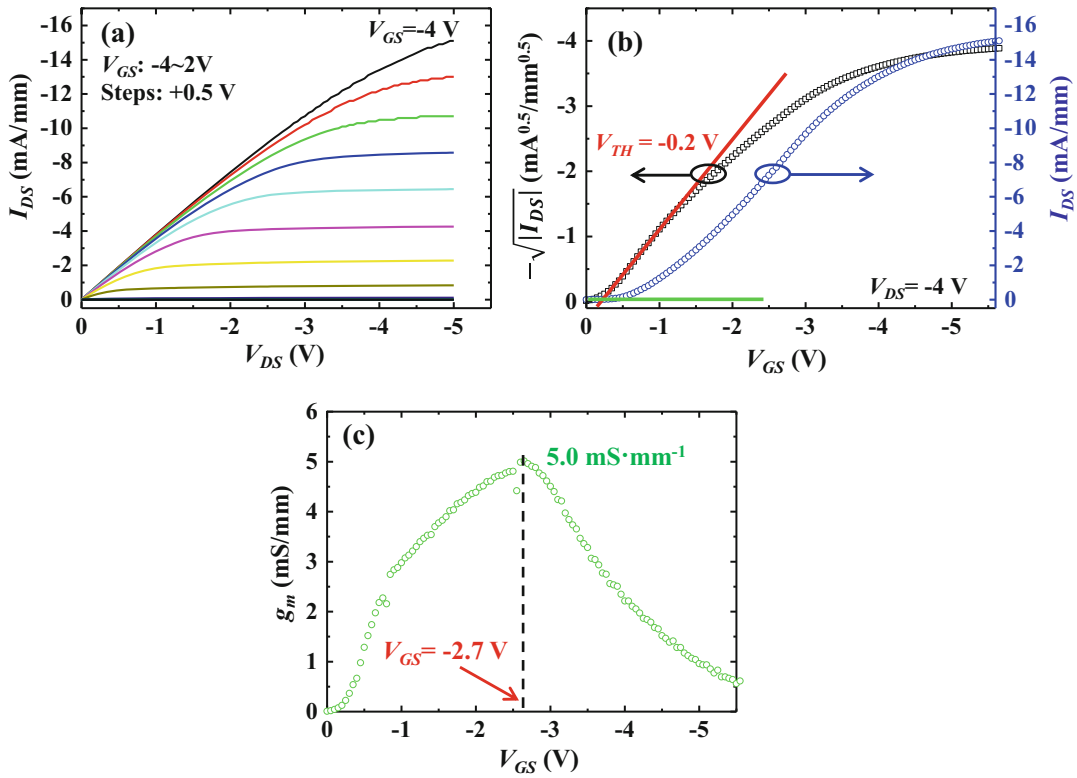

Fig. 9 (**a**) I_{DS}-V_{DS} characteristic of the SD-HfO_2/ALD-HfO_2/H-diamond MISFET, (**b**) transfer characteristic corresponding to I_{DS}-V_{DS}, and (c) g_m-V_{GS} characteristic for the MISFET

with normally off characteristic. The on–off ratio at the V_{DS} of −4 V is larger than 10^9

b. The extrinsic transconductance (g_m) as a function of V_{GS} is shown in Fig. 9c. The extrinsic transconductance maximum is found to be 5.0 ±0.1 mS/mm.

4 Notes

1. The treatment of diamond substrate using acid solutions should be carried out in a chemical hood.
2. During diamond substrate treatment, the mixture of HNO_3 and H_2SO_4 solutions produces heat. Therefore, the beaker volume should be larger than 150 ml. The total volume of the HNO_3 and H_2SO_4 solutions is better lower than 40 ml.
3. During diamond surface treatment using acid solutions, the beaker should be covered by a watch glass.
4. Growth conditions usually vary slightly for different MPCVD systems.

5. If the deposition temperature for the H-diamond is higher than 940 °C, the surface of the H-diamond may become rough.
6. The flow rate of the CH_4 can be changed. When the flow rate is higher than 0.5 sccm, the deposition rate of the diamond epitaxial layer may increase. On the other hand, when the flow rate is lower than 0.5 sccm, the deposition rate may decrease.
7. If the growth time is longer than 5 hours, the surface of the H-diamond may become rough.
8. During the growth of H-diamond epitaxial layer, the reflected power and the substrate temperature should be checked and adjusted.
9. Using only the plasma to treat the diamond in ambient H_2 will also produce surface conductivity for the diamond substrate. However, the resistance may be higher than that for H-diamond grown using CH_4 and H_2.
10. There are two necessary conditions for hole accumulation on the H-diamond surface. One is the formation of carbon–hydrogen (C–H) bonds. The other is the adsorbed acceptors on the surface of H-diamond. After taking the H-diamond out of the MPCVD chamber it is necessary to wait a few minutes to form the surface adsorbates.
11. The bilayer photoresists have a AZ5214E/LOR5A bilayer structure. The evaporated metals on the bilayer photoresists can be lifted-off more easily than that on the single layer photoresist.
12. The position accuracy of the laser lithography system is ± 1 μm. Therefore it is difficult to fabricate the MISFET with an L_G thinner than 2 μm.
13. If the photoresist is not removed totally, the sample should be developed again. The developing time is around 1.5 min.
14. During the mesa-structure formation, the etching time should be no longer than 6 min. If the etching time is too long, the photoresists will be etched totally.
15. After using the CCP dry-etching system, the chamber should be cleaned using O_2 gas for 15 min.
16. The three heating steps and long waiting time for the $Hf[N(C_2H_5)CH_3]_4$ precursor is necessary in order to avoid damage during rapid heating.
17. The slight change of pulse and purge times will not affect the quality of the HfO_2 film.
18. After deposition of ALD-HfO_2 film, the ALD chamber should be cleaned by N_2 gas for 20 min.

19. Before the SD-HfO_2 deposition, the sample should be sheltered.
20. In order to check the ALD and SD deposition rates, the ALD-HfO_2 and SD-HfO_2 films are deposited on the silicon substrates, and their thicknesses measured by Ellipsometer.
21. Before metal evaporation the sample should be sheltered.
22. The chamber pressure during evaporation is in the range of 1.0×10^{-5}~3.0×10^{-5} Pa.
23. Since the source/drain ohmic contact is easily removed from the H-diamond surface at high temperature, the lift-off process should be performed at room temperature.
24. During sample cleaning using syringe, the sample should be fixed by a tweezer.
25. During the sample cleaning using acetone and ethanol, please do not use ultrasonic cleaner.

Acknowledgments

This work was supported by International Center for Young Scientists (ICYS) of the National Institute for Materials Science (NIMS). It was also supported in part by the Tokodai Institute for Elemental Strategy (TIES), Advanced Environmental Materials, Green Network of Excellence (GRENE), and a Fundamental Research A (No. 25249054) project sponsored by the Ministry of Education, Culture, Sports, and Technology (MEXT), Japan. The authors thank Dr. M. Y. Liao and Dr. M. Imura in the Wide bandgap Materials Group, and Mr. H. Oosato, Dr. E. Watanabe, and Dr. D. Tsuya in the Nanotfabrication Platform of NIMS for their helps on the fabrication of the H-diamond MISFETs.

References

1. Bergveld R, Wiersma J, Meertens H (1976) Extracellular potential recordings by means of a field effect transistor without gate metal, called OSFET. IEEE Trans Biomed Eng 23:136–144
2. Im H, Huang X, Gu B, Choi Y (2007) A dielectric-modulated field-effect transistor for biosensing. Nat Nanotech 2:430–434
3. Sato H, Kasu M (2013) Maximum hole concentration for hydrogen-terminated diamond surfaces with various surface orientations obtained by exposure to highly concentrated NO_2. Diamond Relat Mater 31:47–49
4. Song K, Zhang G, Nakamura Y, Furukawa K, Hiraki T, Yang J, Funatsu T, Ohdomari I, Kawarada H (2006) Label-free DNA sensors using ultrasensitive diamond field-effect transistors in solution. Phys Rev E Stat Nonlin Soft Matter Phys 74:041919
5. Dankerl M, Eick S, Hofmann B, Hauf M, Ingebrandt S, Offenhausser A, Stutzmann M, Garrido JA (2009) Diamond transistor array for extracellular recording from electrogenic cells. Adv Funct Mater 19:2915–2923
6. Liu JW, Liao MY, Imura M, Koide Y (2013) Normally-off HfO_2-gated diamond field effect transistors. Appl Phys Lett 103:092905
7. Liu JW, Liao MY, Imura M, Tanaka A, Iwai H, Koide Y (2014) Low on-resistance hydrogenated-diamond field effect transistors with high-k ZrO_2/Al_2O_3 bilayer as dielectric. Sci Rep 4:6395